# Effect of support acidity during selective hydrogenolysis of glycerol over supported palladium ruthenium catalysts

**Susana Guadix-Montero,[a] Alba Santos-Hernandez,[a]**

**Andrea Folli[b], Meenakshisundaram Sankar[a*]**

[a] *Cardiff Catalysis Institute, School of Chemistry, Cardiff University, Cardiff, CF10 3AT, United Kingdom.*
[b] *School of Chemistry, Cardiff University, Cardiff, CF10 3AT, United Kingdom*
*ORCID ID*

**Keywords:** Glycerol, hydrogenolysis, support, bimetallic, bifunctional catalyst,

## Summary

We report the role of the acidity of support during the selectivity hydrogenolysis of glycerol over supported bimetallic palladium-ruthenium catalysts. The PdRu nanoparticles were supported on a series of metal oxides and zeolitic supports *via* the modified impregnation method and tested for the liquid-phase hydrogenolysis of glycerol using gaseous hydrogen. The relative acid site densities of selected catalysts were determined by ammonia temperature-programmed desorption and pyridine desorption experiments. Based on these studies, we report a direct correlation between the catalytic activity (conversion & 1,2 propane diol yield) and two different acid sites (strong acid sites and very strong acid sites). Besides zeolite supported catalysts, $TiO_2$ supported PdRu nanoparticles exhibits moderate catalytic activity however, this catalyst shows high selectivity for the desired C-O bond cleavage to produce C3 products over the undesired C-C bond cleavage to produce < C3 products.

## Introduction

Biodiesel is the largest fraction of biofuels produced in Europe, accounting for nearly 37 % of the global production.[1] The transesterification process to produce biodiesel from triglycerides generates large quantities of crude glycerol as a by-product.[2-6] Because of the abundance, and the fact that glycerol is produced as a waste, it has been identified as one of the important bio-derived platform molecules to produce chemicals.[4-6] Economically, catalytic hydrogenolysis of glycerol to C3 diols, such as propanediols, is an attractive transformation.[7, 8] However, designing heterogeneous catalysts that are selective for the hydrogenolysis of C-O bonds without breaking the C-C bonds to produce C3 products remains a challenge. Several products are potentially possible during the hydrogenolysis of glycerol (Scheme -1), hence, achieving high selectivity towards the desired product is key. Many supported metal nanoparticles have been reported for the selective hydrogenolysis of glycerol to propane diols using $H_2$.[7] In heterogeneous catalysis, using supported metal catalysts, support materials play a crucial role in dispersing and stabilising the active metal components and thereby increasing and stabilising the active metal surface area.[9] Hence, it is vital to investigate and understand the relationship between support property and catalytic activity to rationally design a catalyst.

*Author for correspondence (sankar@cardiff.ac.uk).
Corresponding author address: Cardiff Catalysis Institute, School of Chemistry
Cardiff University, Cardiff, CF10 3AT, United Kingdom.

A number of noble (Ru, Rh, Pd, Ir, Pt, Re, Ag, Au) and non-noble (Co, Ni, Cu, Zn, Al, Fe, Mg, Si) metal nanoparticles supported on activated carbon (including graphite and carbon nanotubes), $Al_2O_3$, $SiO_2$, zeolites and metal oxides have been reported as effective catalysts for glycerol hydrogenolysis.[7, 10-19] These reports mainly indicate that metallic sites and acidic sites catalyse hydrogenation and dehydration reactions respectively. Bifunctional catalysts, having metallic sites and acid sites favour the formation of C3 products, however it is critical to selectively break the C-O bonds without affecting the C-C bonds.[17, 20, 21] This could be accomplished by the tuning of the acid sites on the catalyst surface. Li *et al.*, reported the beneficial effect of the acidity of the catalyst during glycerol hydrogenolysis. They demonstrated this by adding acidic $ReO_x$ to Pd to improve the catalytic activity of Pd catalyst.[22] Support materials play important role in the stability of the catalyst as well. For instance, in the case of supported monometallic Ru catalyst, $Al_2O_3$ gave a more stable catalyst compared to $SiO_2$. Both $Al_2O_3$ and $SiO_2$ supported catalysts were, however, outperformed by activated carbon supported catalyst.[7] Delgado *et al.* showed that when $TiO_2$ supported catalysts were more selective towards C-O bond cleavage over C-C bond cleavage resulting in higher C3 products.[20] In spite of these reports, the relationship between support property and the catalytic property is still an interesting area of research.

Since Ru-based catalysts are found to be extremely active for this reaction, bimetallic palladium ruthenium nanoparticles-based catalysts have been selected to study the role of the acidity on the products selectivity. In an earlier report, we reported that bimetallic PdRu nanoparticles are more selective, compared to the monometallic Ru nanoparticles, for the hydrodeoxygenation of levulinic acid to γ-valerolactone.[23] In this work, zeolites with different framework and $SiO_2$ / $Al_2O_3$ ratio have been used to support bimetallic PdRu nanoparticles. Besides to these zeolitic supports, pure metal oxides as $SiO_2$, $Al_2O_3$, $TiO_2$ and a novel mixed metal oxide ($TiO_2$ doped with ca. 10%$_{at}$ of W, ($Ti_{0.9}W_{0.1}O_2$)) were also used as supports for the bimetallic Pd nanoparticles. From the catalytic data of all these catalysts, along with their characterisation data, we report the relationship between support acidity and the catalytic property of these multifunctional supported PdRu bimetallic catalysts for the selective hydrogenolysis of glycerol.

# Experimental

**Preparation of bimetallic catalyst**

2 wt.% PdRu bimetallic nanoparticles were supported on different metal oxides ($SiO_2$, $Al_2O_3$, $WO_3$ from Sigma Aldrich) and zeolites. Commercial zeolites were purchased from Alfa Aesar and had different $SiO_2/Al_2O_3$ ratios and frameworks such as $NH_4$-ZSM-5 ([30:1], [50:1], [80:1] and [400-200:1]), $NH_4$-Mordenite [20:1] and HY [5.1:1]. The commercial zeolites in the ammonium-ion form ($NH_4^+$-forms) were pre-treated by calcination at 550 °C for 4 h (heating rate of 10 °C min $^{-1}$) under flowing air to form the $H^+$ form. This $H^+$ form of the zeolites were used for supporting the PdRu nanoparticles. The mixed metal oxide $Ti_{0.9}W_{0.1}O_2$ was prepared *via* an already reported sol-gel route and the detailed synthesis procedure is reported elsewhere.[24] The metal oxides were used without any further heat treatments for supporting the PdRu nanoparticles. Supported bimetallic PdRu nanoparticles were prepared *via* a modified impregnation method.[23, 25] A 2 wt. % PdRu/Support catalyst with equimolar metal loadings of the two metals was prepared *via* the following procedure. An aqueous solution of $PdCl_2$ was prepared with a metal concentration of 6 mg$_{Pd}$ mL$^{-1}$ in a 0.58 M HCl solution. An aqueous solution of $RuCl_3.xH_2O$ with a metal concentration of 6.7 mg$_{Ru}$ mL$^{-1}$ was also prepared separately. Requisite amounts of metal precursor solutions were added to a 50 mL round-bottom flask fitted with a magnetic stirrer bar. The additional volume of deionised water was added to make the total volume of the impregnation mixture to 16 mL. The support (1.98 g) was added slowly over a period of 15-20 min with constant vigorous stirring at 60 °C. Then it was stirred for an additional 15 min, followed by an increase in the synthesis temperature to 95 °C. The slurry was stirred overnight at 95 °C until all the water evaporates (typically 16 h). The resultant dry powder was ground thoroughly and reduced under a flow of 5 % vol. $H_2$/Ar at 400 °C for 4h with a heating rate of 10 °C min$^{-1}$.

**Glycerol hydrogenolysis aqueous phase reaction.**

The catalytic activities of the supported bimetallic nanoparticles were tested in a 50 mL stainless-steel autoclave (Parr® Instruments) with a maximum operating pressure of 2000 psi for the hydrogenolysis of glycerol using molecular hydrogen. This autoclave reactor was equipped with an overhead stirrer (0-1500 rpm). The reaction temperature was monitored using a thermocouple and the reactor pressure was measured using a transducer. Initially, the reactor was charged with an aqueous solution (24 mL of 5 wt. % aqueous glycerol solution) and the catalyst was added to the reactor. The substrate to the total metal molar ratio was always kept at 1:0.005 unless stated otherwise. Initially, the autoclave was purged three times with $N_2$ (10 bar) followed by further purging with $H_2$ (20 bar) twice before being pressurised at 20 bar at 25 °C. The reaction mixture was stirred below 200 rpm until the reaction temperature reached 165 °C, after which the stirring rate was increased to 800 rpm. This moment was considered as the starting of the reaction (*t = 0*). At the end of the reaction, the reactor was cooled down to 10 °C in an ice bath. The gas-phase was collected in a gas sampling bag and injected in a Varian 450 Gas Chromatograph (GC), fitted with a Varian Capillary Column CP-Sil 5 CB 50 m 0.32 mm 5 μm, for the quantitative analyses of the gaseous products. The solid catalyst was removed from the liquid reaction mixture by centrifugation at 4300 rpm for 20 min. Further filtration using 0.45 μm PTFE syringe filters, ensured even the finest catalytic particles were removed from the liquid. The separated liquid reaction mixture was then injected in an Agilent 7820A GC fitted with an Agilent DB-WAX Ultra Inert GC column and a flame ionization detector. A fixed amount of n-butanol was used as an external standard for quantitative analyses. Conversion, selectivity and total carbon mass balance (CMB (T)) were calculated using the following equations:

$$Conversion\ (\%) = \frac{(mol_{glycerol})_{t=0} - (mol_{glycerol})_{t=t}}{(mol_{glycerol})_{t=0}}\ \text{X}\ 100$$

$$Selectivity_P\ (\%) = \frac{mol_P}{\sum mol\ of\ all\ products}\ \text{X}\ 100$$

$$Total\ carbon\ mass\ balance\ (\%) = \frac{\sum mol_{C1\ products} + 2 \cdot \sum mol_{C2\ products} + 3 \cdot \sum mol_{C3\ products} + 3 \cdot (mol_{glycerol})_{t=t}}{3 \cdot (mol_{glycerol})_{t=0}}\ \text{X}\ 100$$

For reusability studies, the solid catalyst was recovered after the reaction, washed with acetone several times and dried at 25 °C overnight. This used catalyst was further dried at 120 °C for 1h and then used in the reusability studies. This dried catalyst was used for further analysis and characterisation.

**Catalyst characterisation**

*Thermogravimetric Analyses*

Thermogravimetric analyses (TGA) of the fresh and spent supported bimetallic PdRu catalysts, were performed on a PerkinElmer Pyris 1 thermogravimetric analyser, under $N_2$ flow (30 mL $min^{-1}$). Initially, the sample was stabilised at 30 °C for 20 min and then the temperature was increased to 800 °C at a rate of 10 °C $min^{-1}$. No gas buoyancy effect corrections were applied for the measurements. In this article, only the relative intensities are reported.

*Transmission Electron Microscopic (TEM) studies*

TEM images of the catalysts were obtained using a JEM-2100F (JEOL) microscope. Prior to the TEM measurements, the samples were dispersed with ethanol under ultrasonication and deposited on 300 mesh copper grids coated with holey carbon film. The supernatant liquid was dropped on a C grid and dried with a lamp before analysis. TEM and STEM were performed on a JEOL JEM-2100 microscope operating at 200 kV.

*Inductively coupled plasma analysis*

The samples for leaching studies were run on an Agilent 7900 ICP-MS with I-AS auto sampler with Platinum Sampling and Skimmer cones, concentric nebulizer and quartz double pass spray chamber. All analyses were run using helium (He mode) and the ORS cell to reduce interferences. For metal content determination in solids, *ca.* 2 mg of catalyst was dissolved in 10 mL aqua-regia for at least 12 h. The final solution was diluted to 50 mL with water in a volumetric flask. In all cases, further dilutions were done if required. All results were done in duplication and further analyses were performed if two results differed.

*Powder X-ray diffraction studies of zeolites*

Powder X-ray diffraction (XRD) patterns of the calcined support materials and the fresh and used 2 wt.% PdRu supported catalysts were collected with a PANanalytical X'Pert Pro ® diffractometer using a copper anode (K$\alpha$ 1.54184 Å) ray source, operating at 40 kV and 40 mA. The signals were collected between the 2$\theta$ values of 5° to 80° with a step of $0.02^0$.

*Ammonia temperature-programmed desorption ($NH_3$-TPD) studies*

$NH_3$-TPD was carried out using a CHEMBET TPR/TPD chemisorption analyser/benchtop from Quantachrome Instruments. The desorption was monitored *via* a thermal conductivity detector (TCD), which senses changes in the thermal conductivity and compares it to the conductivity of the carrier gas (Helium). A calibration plot was obtained by the integration of the peak area for different injection volumes of pure ammonia (Figure S1). The flow of carrier gas (helium) was set between 50-100 mL $min^{-1}$. For quantification of the acid site density, approximately 0.05-0.1 g of the material was added in a U-shape quartz tube and was packed between two quartz wool plugs. Sample pre-treatment was performed at 130 °C for 1h (heating rate of 15 °C $min^{-1}$) to remove the water content. After pre-treatment, the material was exposed to a constant flow of 10% ammonia in argon for 30 min. Then the sample was heated up to 100 °C ( rate of heating = 15 °C $min^{-1}$) and held at this temperature for 1 h to remove the physisorbed $NH_3$. Finally, the desorption programme was initialised by setting a heating rate of 15 °C $min^{-1}$ up to 800 °C and 5 min hold time. The relative acidity of the catalyst was estimated using the following equation.

$$Acidity\ (NH_3\ \mu mol\ g^{-1}) = (\frac{Area\ acid\ site}{RF\ NH_3 calibration})/g_{catalyst}$$

Least square fitting of the $NH_3$-TPD results to a Gaussian line shape was performed for all the catalysts and the results are presented in the Supplementary Information. The goodness of the fit was estimated by $\chi^2$ , reduced $\chi_\nu{}^2$, residual sum of squares (RSS) and correlation coefficient ($R^2$). Different methods have been reported to quantify the acid sites of a catalyst.[26] In this work, four peaks have been identified and are assigned as follows: peak around 250 °C for weak acid sites; peak around 330 °C for medium acid sites; peak around 430 °C for strong acid sites and finally the peak around 530 °C for very strong acid sites. These peaks have been deconvolved for semi-quantitative analyses. Gaussian peak fitting has recently been used to quantify the acidity of zeolites, such as ZSM-5, HY, Beta, and Mordenite.[27-31] Here, we employ the same strategy to quantify the acid sites. In some cases, this method was applied to deconvolute the experimental curve even in six fixed temperature ranges to get a good fit and a better comparison between samples.[32]

*Diffuse Reflectance Infrared Fourier Transform Spectroscopy (DRIFTS)*

The samples were pre-treated at 110 °C overnight in a conventional oven prior to the analysis. The instrument employed was a Bruker Tenso27 FT-IR spectrometer equipped with a mercury-cadmium-telluride (MCT)-detector, cooled down using liquid $N_2$. The IR source was a mid-Infrared (MIR) source and with a standard KBr beam splitter, which had a range of 7500-370 $cm^{-1}$. *In-situ* heating was carried out in a Harrick Praying Mantis high-temperature diffuse reflection chamber (HVC-DRP-4) *in-situ* cell at 500 °C for 2 hours under flowing $N_2$ (40 mL $min^{-1}$) adjusted using a Brooks mass flow controller (MFC). After pre-treatment, a background spectrum was recorded at 30 °C and was used for background correction for each measurement.

Pyridine was then absorbed by exposing the sample for 5 min to a flow of 50 mL min $^{-1}$ of $N_2$ bubbling into pyridine through a heated line at 110 °C. The excess of pyridine was removed by vacuum for 5 min. The IR spectra were collected while heating the sample from 30 to 575 °C. 5 scans were taken after 5 min of reaching the desired temperature, to have a stable measurement. The spectra were recorded between 4000 cm$^{-1}$ and 1000 cm$^{-1}$ with a 2 cm$^{-1}$ frequency.

# Results and discussion

**Catalytic activity**

2 wt.%PdRu nanoparticles supported on different supports were tested for glycerol hydrogenolysis under standard reaction conditions and the results, presented in Table -1 and Table -2, show the crucial role of support on the catalytic activity. Among all the supports tested, ZSM-5 (Entries 5, 6 and 7 in Table -1) gave higher conversion, however, these catalysts gave lower selectivity to liquid products, as evidenced from the carbon mass balance for liquid products CMB (L) in *Figure* 1. From the same set of data, it is evident that, for a given zeolite (ZSM), the Si/Al ratios from 30:1 to 80:1 the catalytic activity increases with the increase in Al content (with an exception for 80:1 catalyst). However this increased activity accompanies a decreased C3 selectivity. Figure S1 in the supporting information shows an increase in C1 products with an increase in the Al content, possibly because of the increased Bronsted acidity for the catalysts containing higher Al content. Table -2 compares the activities of catalysts with metal oxide supports against the zeolites supported catalysts. It is clear that zeolites are more active supports compared to pure metal oxides because of the presence of more acidic sites on zeolites compared to pure metal oxides. However, these acid sites promote C-C bond cleavage resulting in undesired <C3 products including gaseous products. It must be noted that $TiO_2$ is a promising support (Table -2, Entry 2) with a reasonably high catalytic activity (55%) and selectivity for liquid products (72%). *Figure* compares the products selectivity at iso-conversion for different supports. At *ca.* 50% glycerol conversion level, (*Figure* -A), PdRu/$TiO_2$ gives a better 1,2-PDO selectivity than PdRu/ZSM-5 (50:1), 50% vs *ca.* 15 % respectively. For the ZSM-5 supported catalyst, $CH_4$ is the major product (49 % selectivity) along with small amounts of other products like 15 % of EG and 8 % of 2-PO.

PdRu nanoparticles supported on other kinds of zeolites such as PdRu/HY (Entry 3 in Table-1) and PdRu/MOR (Entry 4 in Table-1) resulted in less than 20% glycerol conversion. The selectivities of these catalysts were compared at a lower conversion levels (*ca.* 20%) (*Figure* -B). The product distribution in the case of PdRu/MOR suggests that it promotes mostly C-C cleavage than C-O cleavage. Priya *et al.* reported monometallic Pt nanoparticles and bimetallic Pt-Cu nanoparticles supported on Mordenite zeolite as effective catalysts for glycerol hydrogenolysis, *albeit* at a much harsher reaction condition.[11, 12] Among other catalysts, PdRu/$TiO_2$ is the most selective catalyst for 1,2-PDO (33 %) at *ca.* 20 % glycerol conversion. Other catalysts resulted in lesser selectivity for 1,2-PDO: PdRu/MOR (17 %), PdRu/ZSM5-200:1 (16 %) and PdRu/$Al_2O_3$ (19 %). All these catalysts showed appreciable selectivity towards EG (between 22-36 %). Importantly, PdRu/$TiO_2$ showed the least selectivity for $CH_4$ (11 %) in comparison to other supports (33-37 %). In summary, for the liquid phase glycerol hydrogenolysis reaction using PdRu bimetallic catalyst supported in different zeolite type frameworks, the activity follows the order ZSM-5 >> MOR [20:1] > HY[5.1:1] which is in partial agreement with the reported trends for glycerol dehydration reaction.[11, 33]

From the previous results, $TiO_2$ is found to be a promising support and it has been reported that addition of $WO_x$ has a positive effect in increasing the selectivity of C3 products during glycerol hydrogenolysis.[34] Based on these two facts, a mixed metal oxide containing both $TiO_2$ and $WO_x$ was prepared ($Ti_{0.909}W_{0.091}O_2$) and used as a support for PdRu nanoparticles. Entry 1 in *Table* 1 shows the results achieved by the 2 wt.% PdRu/$Ti_{0.9}W_{0.1}O_2$ catalyst. It gave the best selectivity to 1,2-PDO, followed by the $SiO_2$ (Entry 9) and $TiO_2$ (Entry 2) supported catalysts. Nevertheless, the conversions in these cases (Entries 1 and 9) were below 10 %. It has been reported that to achieve good 1,2-PDO selectivity the presence of moderate strength of Lewis acidity is required.[35] Based on that hypothesis, $SiO_2$ has widely been used as a support for this reaction. For example,

RuRe/$SiO_2$ catalyst gave an excellent 1,2-PDO selectivity.[36] In this case, the bifunctional nature of the catalyst having both Re oxide (acidic sites) to the Ru metal sites resulted in the excellent activity and selectivity (51 % of conversion and 25 % selectivity) however, with a high metal loading (9 wt. %). In our system, at low conversion levels (*ca.* 15 %), *Figure* 1-C shows that the 1,2-PDO selectivity follows the order PdRu/$Ti_{0.9}W_{0.1}O_2$ (49 %) >PdRu/$TiO_2$ (40 %) > PdRu/HY (22 %).

The hydrogenolysis reactions were run at a much lower conversion levels (<10%) to compare the selectivity between $Ti_{0.9}W_{0.1}O_2$ supported catalyst and the $SiO_2$ supported catalyst. PdRu/$Ti_{0.9}W_{0.1}O_2$ gave the highest selectivity for 1,2-PDO (82 %) and the lowest selectivity of EG (3 %) at a glycerol conversion of *ca.* 7 % (*Figure* - D). In comparison, the PdRu/$SiO_2$ resulted in a much lesser 1,2-PDO selectivity (42 %) whereas the selectivity to EG was higher (28 %). Another C3 alcohol (1-propanol), produced from the hydrogenolysis of 1,2-PDO (see *Scheme* 1), is also detected in all the reactions. The production of 1-PO *via* the hydrogenolysis of 1,2-PDO under relatively mild conditions has been reported.[37] This type of consecutive hydrogenolysis is one of the reasons for the difficulty in achieving high conversion of glycerol and high selectivity of 1,2-PDO at longer reaction times.[7, 34, 38-40] In our investigation, most of the catalysts showed relatively higher selectivity to propane after 16 h reaction (*Table* 2 and *Figure* -C) which supports this. At much longer reaction times, i.e. 16 h (*Table* 2), the activities of PdRu/$Ti_{0.9}W_{0.1}O_2$, PdRu/$SiO_2$ and PdRu/$Al_2O_3$ were around 12, 22 and 7 % respectively. Overall, the results indicate that $TiO_2$, which gives around 55 % of conversion and 50 % of 1,2-PDO selectivity seems to be a promising support.

**Catalyst characterisation and stability.**

During the synthesis of PdRu supported on zeolites, there is a possibility for the complete or partial collapse of the zeolitic structure.[41-43] This is also possible during the catalytic reaction as well. To study the stability the zeolitic materials during the catalyst synthesis and during the reaction, the calcined supports prior to metal impregnation, fresh catalysts and spent catalysts were characterised by powder XRD (Figure 3). The results show the characteristic reflections corresponding to each framework for the calcined samples.[44] All the ZSM-5 and the MOR materials exhibit no significant changes in the zeolite framework for the fresh catalysts and the spent catalysts.[42] This indicates that these zeolitic structures are stable during the metal impregnation and during the catalytic reaction. This observation is expected since, during modified impregnation method, the metal cations are not incorporated into the zeolite framework, but at the external surface or even inside the pores of the zeolite, as mentioned earlier.[45] However, for the used catalyst PdRu/HY zeolite the peak intensities are lesser than the fresh catalyst suggesting a *ca.* 85 % reduction in the crystallinity of its original level of the Zeolite Y (FAU type) after the reaction. This degradation is in line with Dimitrijevic *et al.* who reported a 60 % loss in crystallinity to produce amorphous material and kaolinite.[46] The XRD data of the rest of catalysts are presented in the Supplementary Information (Figure S2)

Leaching of the catalyst components during the hydrogenolysis reaction was studied using inductively coupled plasma (ICP) method. The amounts of different metals present in the reaction mixture, quantified by ICP, are given in *Figure* 4. The results show that Si leaching was observed for all the zeolite supported catalysts, typically less than 8 %. Significant PdRu leaching (*ca.* 5%) was observed only in the case of $Al_2O_3$ supported catalyst. Among the zeolite supported catalysts, PdRu/ZSM-5 catalyst with 80:1 molar ratio of Si:Al showed some Ru and Pd leaching (less than 1.5 % of Ru and about 1 % of Pd). However, no significant Pd leaching was observed for PdRu/ZSM-5 and PdRu/$TiO_2$ catalysts.

TEM images of selected catalysts (Figure S3) reveal well-dispersed spherical metal nanoparticles. Selected area electron diffraction (SAED) patterns showed continuous ring-like patterns for both HY (A2) and Mordenite (B2) supported catalyst. These patterns indicate that the catalysts have finer nanoparticle size and weaker crystallinity than the ZSM-5 supported catalysts. ZSM5 zeolites with different Si/Al ratios show more evident and speckled patterns (C2, D2, E2 and F2). Since we have used the well studied modified impregnation

methodology for preparing these supported bimetallic catalysts, we believe that these bimetallic particles form a homogeneous random alloy structure. Earlier studies on similar catalysts using STEM-XEDS and XAS have shown that Ru and Pd form a homogeneous random alloy structure.[23]

To study whether coking or irreversible adsorption of substrate and/or products occurs on the catalysts, thermogravimetric analyses (TGA) of the fresh and the spent catalyst were performed. From the TG thermograms represented in Figure S4, it can be observed that < 10 wt. % weight loss for the fresh and spent catalyst was obtained below 200 °C. Besides this, there is no appreciable between the fresh and spent catalysts. These results clearly show that spent catalysts do not have any coke or irreversibly adsorbed substrate or products.

**Effect of catalysts acidity on hydrogenolysis of glycerol.**

Since acidity of the catalyst is an important property for glycerol hydrogenolysis reaction, relative acid site densities of the samples were determined by $NH_3$-TPD.
*Figure* compares the acid site densities for all the PdRu/support catalysts used. PdRu/MOR and PdRu/ZSM-5 (30:1) have the highest total acid sites among all the catalysts. Total acidity may not be an important property for this reaction. Hence, Lewis and Brønsted acidity of the most active catalyst (PdRu/ZSM-5 (80:1)) and the most acidic catalyst (PdRu/MOR) were measured using pyridine desorption *via* DRIFTS. For the identification and quantification of different acid sites, we focused on the frequency range from 1600 to 1400 $cm^{-1}$. In this region, the band at 1540 $cm^{-1}$ correspond to the C-C bond vibration of the pyridinium ion and this can be used to identify and quantify Brønsted acid sites.[47] The Lewis acid sites can be identified and quantified using the band at 1450 $cm^{-1}$, while the band at 1490 $cm^{-1}$ correspond to both Brønsted and Lewis acid sites.[11] It is known that the impregnation of metal results in a decrease in the amount of the Brønsted sites, however, it increases the Lewis acid sites, the metal sites act as Lewis acid sites by accepting electron pairs from pyridine. *Figure* 6 shows two different FTIR spectra of pyridine adsorbed on a) ZSM-5 and b) MOR zeolites (from 30-575 °C). It can be seen how the peaks reduce their intensity along with the temperature increases until no pyridine remains absorbed at 300 °C. The nature of the acid sites is compared for the most active ZSM-5 (80-1) (*Figure* 6-a) with the most acid support Mordenite (*Figure* 6-b). The results indicate that PdRu/MOR contains more Brønsted acid sites than Lewis acid sites. In the case of the PdRu/ZSM-5, the opposite was found. Yoda *et al.* studied the reaction pathways for the dehydration of glycerol over H-ZSM-5, confirming that different kind of acid sites catalyse different reaction pathways.[48] Lewis acid sites favours the dehydration pathway A (*Scheme* 1). Lewis sites attack the primary hydroxyl group to form 1,2-PDO via acetol. On the contrary, Brønsted acid sites favour the mechanism pathway B, interacting with the secondary hydroxyl group of glycerol (*Scheme* 1).[18, 48, 49] This could be the main reason why the PdRu/ZSM-5 catalyst results in high glycerol conversion with highest 1,2-PDO selectivity compared to PdRu/MOR catalyst.

This conclusion from the pyridine adsorption studies that PdRu/MOR catalyst has more Brønsted acid sites compared to PdRu/ZSM-5 catalyst agrees with the $NH_3$ desorption results as well. In the $NH_3$-TPD data, the two low temperature peaks are assigned to weak Brønsted and Lewis sites, whereas the peaks above 450 °C are assigned to strong and very strong Brønsted acid sites respectively. Based on this, two plots are presented in Figure 7. Figure 7A shows the correlation between strong acidity of the catalyst *vs* conversion/$CH_4$ yield and 1,2-PDO yield for a few selected catalysts. Figure 7B shows a similar correlation between very strong acidity of the catalyst *vs* conversion/$CH_4$ yield and 1,2-PDO yield. Both plots show a volcano type curve. These plots show a maximum activity around 40 $NH_3$ μmol $g^{-1}$ of very strong and 130 $NH_3$ μmol $g^{-1}$ of strong acid sites for the PdRu/ZSM-5 (80:1) catalyst, with a glycerol conversion of *ca.* 75 %. It is important to note that PdRu/$TiO_2$, which produces least amount of $CH_4$, contains almost the same amount of strong acid sites. This agrees with Patri and co-workers who reported that $TiO_2$ showed the best results for their AuPt bimetallic catalysts: (AuPt/$TiO_2$) > (AuPt/MCM41 ≥ AuPt/ $SiO_2$) > (AuPt/H-Mordenite > AuPt/S-$ZrO_2$).[35]

# Conclusions

To conclude this work demonstrates the correlation between the different acid sites of the PdRu/support catalysts and their catalytic properties for the aqueous phase glycerol hydrogenolysis. ZSM-5 with Si:Al ratio of 30:1, 50:1 and 80:1 displayed the highest catalyst activity and stability. However, these catalysts have higher proportion of Lewis acid sites with lesser Brønsted acid sites as evidenced by the pyridine DRIFTS data. Consequently, these catalysts yield more 1,2-PDO than 1,3-PDO among the liquid products. These catalysts also produced substantial amounts of $CH_4$ produced via a C-C bond cleavage. It was found that the strong acidity of these materials correlates with their activity showing a volcano plot. Among the supports tested, $TiO_2$ has moderate acidity and showed excellent catalytic activity producing 1,2-PDO and producing least amount of C1 products, such as $CH_4$. The simultaneous presence of bimetallic noble metals and moderate density of strong acid sites favour the yield to C3 products. It must be noted that the nature of support (including textural properties) can also influence the nanostructure of the metal nanoparticles and hence the active sites for this reaction. Further detailed characterisation is needed to study this correlation.

**Acknowledgments & Funding Statement**
SGM thanks Cardiff University for her PhD studentship. MS thanks Cardiff University for his University Research Fellowships. AS thanks the EPSRC for her PhD studentship through the CDT in Catalysis.

**Data Accessibility**
The datasets supporting this article have been presented as Supplementary Material. In addition to that, the meta data relevant to this study are presented in http://doi.org/10.17035/d.2020.0106627295.

**Competing Interests**
Authors have no competing interests.

**Authors' Contributions**
SG and AS synthesized all the catalysts and performed all the experimental work under the supervision of MS. AF synthesized and characterised the $Ti_{0.9}W_{0.1}O_2$ material. All authors contributed equally to the analysis of the data and drafting of this article. MS directed this project.

# References

[1] Xu, J. & Li, M. 2017 Innovative technological paradigm-based approach towards biofuel feedstock. *Energy Conversion and Management* **141**, 48-62. (doi:https://doi.org/10.1016/j.enconman.2016.04.075).
[2] Luo, X., Hu, S., Zhang, X. & Li, Y. 2013 Thermochemical conversion of crude glycerol to biopolyols for the production of polyurethane foams. *Bioresource Technology* **139**, 323-329. (doi:https://doi.org/10.1016/j.biortech.2013.04.011).
[3] Hunsom, M. & Saila, P. 2015 Electrochemical conversion of enriched crude glycerol: Effect of operating parameters. *Renewable Energy* **74**, 227-236. (doi:https://doi.org/10.1016/j.renene.2014.08.008).
[4] Chatwani, B.N. & Mewada, R.K. 2013 Development of Rate Expression for Glycerol Hydrogenation Reaction. *Procedia Engineering* **51**, 443-450. (doi:https://doi.org/10.1016/j.proeng.2013.01.062).
[5] Kim, Y.C. & Moon, D.J. 2019 Sustainable Process for the Synthesis of Value-Added Products Using Glycerol as a Useful Raw Material. *Catalysis Surveys from Asia* **23**, 10-22. (doi:10.1007/s10563-018-09263-z).
[6] ten Dam, J. & Hanefeld, U. 2011 Renewable Chemicals: Dehydroxylation of Glycerol and Polyols. *ChemSusChem* **4**, 1017-1034. (doi:10.1002/cssc.201100162).
[7] Nakagawa, Y. & Tomishige, K. 2011 Heterogeneous catalysis of the glycerol hydrogenolysis. *Catalysis Science & Technology* **1**, 179-190. (doi:10.1039/C0CY00054J).
[8] Gilkey, M.J. & Xu, B. 2016 Heterogeneous Catalytic Transfer Hydrogenation as an Effective Pathway in Biomass Upgrading. *ACS Catalysis* **6**, 1420-1436. (doi:10.1021/acscatal.5b02171).

[9] Misono, M. 2013 Chapter 5 - Mixed Oxides as Catalyst Supports. In *Studies in Surface Science and Catalysis* (ed. M. Misono), pp. 157-173, Elsevier.
[10] Furikado, I., Miyazawa, T., Koso, S., Shimao, A., Kunimori, K. & Tomishige, K. 2007 Catalytic performance of Rh/SiO2 in glycerol reaction under hydrogen. *Green Chemistry* **9**, 582-588. (doi:10.1039/B614253B).
[11] Priya, S.S., Bhanuchander, P., Kumar, V.P., Bhargava, S.K. & Chary, K.V.R. 2016 Activity and Selectivity of Platinum–Copper Bimetallic Catalysts Supported on Mordenite for Glycerol Hydrogenolysis to 1,3-Propanediol. *Industrial & Engineering Chemistry Research* **55**, 4461-4472. (doi:10.1021/acs.iecr.6b00161).
[12] Priya, S.S., Bhanuchander, P., Kumar, V.P., Dumbre, D.K., Periasamy, S.R., Bhargava, S.K., Lakshmi Kantam, M. & Chary, K.V.R. 2016 Platinum Supported on H-Mordenite: A Highly Efficient Catalyst for Selective Hydrogenolysis of Glycerol to 1,3-Propanediol. *ACS Sustainable Chemistry & Engineering* **4**, 1212-1222. (doi:10.1021/acssuschemeng.5b01272).
[13] Wang, Y., Zhou, J. & Guo, X. 2015 Catalytic hydrogenolysis of glycerol to propanediols: a review. *RSC Advances* **5**, 74611-74628. (doi:10.1039/C5RA11957J).
[14] Chheda, J.N., Huber, G.W. & Dumesic, J.A. 2007 Liquid-Phase Catalytic Processing of Biomass-Derived Oxygenated Hydrocarbons to Fuels and Chemicals. *Angewandte Chemie International Edition* **46**, 7164-7183. (doi:10.1002/anie.200604274).
[15] Gandarias, I., Requies, J., Arias, P.L., Armbruster, U. & Martin, A. 2012 Liquid-phase glycerol hydrogenolysis by formic acid over Ni–Cu/Al2O3 catalysts. *Journal of Catalysis* **290**, 79-89. (doi:https://doi.org/10.1016/j.jcat.2012.03.004).
[16] Roy, D., Subramaniam, B. & Chaudhari, R.V. 2010 Aqueous phase hydrogenolysis of glycerol to 1,2-propanediol without external hydrogen addition. *Catalysis Today* **156**, 31-37. (doi:https://doi.org/10.1016/j.cattod.2010.01.007).
[17] Chaminand, J., Djakovitch, L.a., Gallezot, P., Marion, P., Pinel, C. & Rosier, C. 2004 Glycerol hydrogenolysis on heterogeneous catalysts. *Green Chemistry* **6**, 359-361. (doi:10.1039/B407378A).
[18] Falcone, D.D., Hack, J.H., Klyushin, A.Y., Knop-Gericke, A., Schlögl, R. & Davis, R.J. 2015 Evidence for the Bifunctional Nature of Pt–Re Catalysts for Selective Glycerol Hydrogenolysis. *ACS Catalysis* **5**, 5679-5695. (doi:10.1021/acscatal.5b01371).
[19] Gallegos-Suarez, E., Guerrero-Ruiz, A., Rodriguez-Ramos, I. & Arcoya, A. 2015 Comparative study of the hydrogenolysis of glycerol over Ru-based catalysts supported on activated carbon, graphite, carbon nanotubes and KL-zeolite. *Chemical Engineering Journal* **262**, 326-333. (doi:https://doi.org/10.1016/j.cej.2014.09.121).
[20] Delgado, S.N., Yap, D., Vivier, L. & Especel, C. 2013 Influence of the nature of the support on the catalytic properties of Pt-based catalysts for hydrogenolysis of glycerol. *Journal of Molecular Catalysis A: Chemical* **367**, 89-98. (doi:https://doi.org/10.1016/j.molcata.2012.11.001).
[21] A, A.A., Mondal, S., Pudi, S.M., Pandhare, N.N. & Biswas, P. 2017 Liquid Phase Hydrogenolysis of Glycerol over Highly Active 50%Cu–Zn(8:2)/MgO Catalyst: Reaction Parameter Optimization by Using Response Surface Methodology. *Energy & Fuels* **31**, 8521-8533. (doi:10.1021/acs.energyfuels.7b00766).
[22] Li, Y., Liu, H., Ma, L. & He, D. 2014 Glycerol hydrogenolysis to propanediols over supported Pd–Re catalysts. *RSC Advances* **4**, 5503-5512. (doi:10.1039/C3RA46134C).
[23] Luo, W., Sankar, M., Beale, A.M., He, Q., Kiely, C.J., Bruijnincx, P.C.A. & Weckhuysen, B.M. 2015 High performing and stable supported nano-alloys for the catalytic hydrogenation of levulinic acid to γ-valerolactone. *Nature Communications* **6**, 6540. (doi:10.1038/ncomms7540).
[24] Bloh, J.Z., Folli, A. & Macphee, D.E. 2014 Adjusting Nitrogen Doping Level in Titanium Dioxide by Codoping with Tungsten: Properties and Band Structure of the Resulting Materials. *The Journal of Physical Chemistry C* **118**, 21281-21292. (doi:10.1021/jp507264g).
[25] Sankar, M., He, Q., Morad, M., Pritchard, J., Freakley, S.J., Edwards, J.K., Taylor, S.H., Morgan, D.J., Carley, A.F., Knight, D.W., et al. 2012 Synthesis of Stable Ligand-free Gold–Palladium Nanoparticles Using a Simple Excess Anion Method. *ACS Nano* **6**, 6600-6613. (doi:10.1021/nn302299e).
[26] Rakić, V. & Damjanović, L. 2013 Temperature-Programmed Desorption (TPD) Methods. In *Calorimetry and Thermal Methods in Catalysis* (ed. A. Auroux), pp. 131-174. Berlin, Heidelberg, Springer Berlin Heidelberg.

[27] Jin, F., Fan, Y.C., Wu, G. & Yuan, M. 2018 Modified Brønsted type equation with ammonia as probe molecule: quantitative acidity-activity relationship for pyridine synthesis with ZSM-5 catalyst. *Reaction Kinetics, Mechanisms and Catalysis* **123**, 517-527. (doi:10.1007/s11144-017-1309-5).
[28] Farahani, S.H., Alavi, S.M. & Falamaki, C. 2017 Improved performance of HZSM-5 for the ethylbenzene/xylene isomerization reaction under industrial operating conditions. *RSC Advances* **7**, 34012-34022. (doi:10.1039/C7RA05924H).
[29] Zou, B., Ren, S. & Ye, X.P. 2016 Glycerol Dehydration to Acrolein Catalyzed by ZSM-5 Zeolite in Supercritical Carbon Dioxide Medium. *ChemSusChem* **9**, 3268-3271. (doi:10.1002/cssc.201601020).
[30] Nuttinee, S., Jatuporn, W., Sanchai, P., Wojciech, S. & Frank, R. 2012 Basic properties of potassium oxide supported on zeolite y studied by pyrrole-tpd and catalytic conversion of methylbutynol. *Química Nova* **35**, 1719-1723.
[31] Zhang, Y., Su, Q., Wang, Z., Yang, Y., Xin, Y., Han, D., Yang, X., Wang, H., Gao, X. & Zhang, Z. 2008 Synthesis and Toluene Adsorption/Desorption Property of Beta Zeolite Coated on Cordierite Honeycomb by an In Situ Crystallization Method. *Chemical Engineering & Technology* **31**, 1856-1862. (doi:10.1002/ceat.200800260).
[32] Bao, Q., Zhu, W., Yan, J., Zhang, C., Ning, C., Zhang, Y., Hao, M. & Wang, Z. 2017 Vapor phase aldol condensation of methyl acetate with formaldehyde over a Ba–La/Al2O3 catalyst: the stabilizing role of La and effect of acid–base properties. *RSC Advances* **7**, 52304-52311. (doi:10.1039/C7RA10008F).
[33] Kim, Y.T., Jung, K.-D. & Park, E.D. 2011 A comparative study for gas-phase dehydration of glycerol over H-zeolites. *Applied Catalysis A: General* **393**, 275-287. (doi:https://doi.org/10.1016/j.apcata.2010.12.007).
[34] Nakagawa, Y., Tamura, M. & Tomishige, K. 2014 Catalytic materials for the hydrogenolysis of glycerol to 1,3-propanediol. *Journal of Materials Chemistry A* **2**, 6688-6702. (doi:10.1039/C3TA15384C).
[35] Villa, A., Manzoli, M., Vindigni, F., Chinchilla, L.E., Botton, G.A. & Prati, L. 2017 Diols Production From Glycerol Over Pt-Based Catalysts: On the Role Played by the Acid Sites of the Support. *Catalysis Letters* **147**, 2523-2533. (doi:10.1007/s10562-017-2183-5).
[36] Ma, L. & He, D. 2010 Influence of catalyst pretreatment on catalytic properties and performances of Ru–Re/SiO2 in glycerol hydrogenolysis to propanediols. *Catalysis Today* **149**, 148-156. (doi:https://doi.org/10.1016/j.cattod.2009.03.015).
[37] Liu, H., Liang, S., Jiang, T., Han, B. & Zhou, Y. 2012 Hydrogenolysis of Glycerol to 1,2-Propanediol over Ru–Cu Bimetals Supported on Different Supports. *CLEAN – Soil, Air, Water* **40**, 318-324. (doi:doi:10.1002/clen.201000227).
[38] Sun, D., Yamada, Y., Sato, S. & Ueda, W. 2016 Glycerol hydrogenolysis into useful C3 chemicals. *Applied Catalysis B: Environmental* **193**, 75-92. (doi:https://doi.org/10.1016/j.apcatb.2016.04.013).
[39] Sun, D., Yamada, Y. & Sato, S. 2014 Production of propanal from 1,2-propanediol over silica-supported WO3 catalyst. *Applied Catalysis A: General* **487**, 234-241. (doi:https://doi.org/10.1016/j.apcata.2014.09.008).
[40] Mai, C.T.Q. & Ng, F.T.T. 2016 Effect of Metals on the Hydrogenolysis of Glycerol to Higher Value Sustainable and Green Chemicals Using a Supported HSiW Catalyst. *Organic Process Research & Development* **20**, 1774-1780. (doi:10.1021/acs.oprd.6b00245).
[41] Viswanadham, N., Saxena, S.K. & Kumar, M. 2011 The Transformation of Light Paraffins to LPG and Aromatics Over a Ni/ZSM-5 Catalyst. *Petroleum Science and Technology* **29**, 393-400. (doi:10.1080/10916460903394037).
[42] Conte, M., Lopez-Sanchez, J.A., He, Q., Morgan, D.J., Ryabenkova, Y., Bartley, J.K., Carley, A.F., Taylor, S.H., Kiely, C.J., Khalid, K., et al. 2012 Modified zeolite ZSM-5 for the methanol to aromatics reaction. *Catalysis Science & Technology* **2**, 105-112. (doi:10.1039/C1CY00299F).
[43] Lai, Y. & Veser, G. 2016 The nature of the selective species in Fe-HZSM-5 for non-oxidative methane dehydroaromatization. *Catalysis Science & Technology* **6**, 5440-5452. (doi:10.1039/C5CY02258D).
[44] Treacy, M.M.J. & Higgins, J.B. 2007 Preface. In *Collection of Simulated XRD Powder Patterns for Zeolites (Fifth Edition)* (eds. M.M.J. Treacy & J.B. Higgins), pp. 1-2. Amsterdam, Elsevier Science B.V.
[45] Fricke, R., Kosslick, H., Lischke, G. & Richter, M. 2000 Incorporation of Gallium into Zeolites: Syntheses, Properties and Catalytic Application. *Chemical Reviews* **100**, 2303-2406. (doi:10.1021/cr9411637).

[46] Dimitrijevic, R., Lutz, W. & Ritzmann, A. 2006 Hydrothermal stability of zeolites: Determination of extra-framework species of H-Y faujasite-type steamed zeolite. *Journal of Physics and Chemistry of Solids* **67**, 1741-1748. (doi:https://doi.org/10.1016/j.jpcs.2006.03.014).
[47] Chow, Y.K., Dummer, N.F., Carter, J.H., Williams, C., Shaw, G., Willock, D.J., Taylor, S.H., Yacob, S., Meyer, R.J., Bhasin, M.M., et al. 2018 Investigating the influence of acid sites in continuous methane oxidation with N2O over Fe/MFI zeolites. *Catalysis Science & Technology* **8**, 154-163. (doi:10.1039/C7CY01769C).
[48] Yoda, E. & Ootawa, A. 2009 Dehydration of glycerol on H-MFI zeolite investigated by FT-IR. *Applied Catalysis A: General* **360**, 66-70. (doi:https://doi.org/10.1016/j.apcata.2009.03.009).
[49] Du, H., Chen, S., Wang, H. & Lu, J. 2017 Acidic alumina overcoating on platinum nanoparticles: Close metal–acid proximity enhances bifunctionality for glycerol hydrogenolysis. *Chinese Journal of Catalysis* **38**, 1237-1244. (doi:https://doi.org/10.1016/S1872-2067(17)62859-6).
[50] Miyazawa, T., Kusunoki, Y., Kunimori, K. & Tomishige, K. 2006 Glycerol conversion in the aqueous solution under hydrogen over Ru/C + an ion-exchange resin and its reaction mechanism. *Journal of Catalysis* **240**, 213-221. (doi:https://doi.org/10.1016/j.jcat.2006.03.023).

**Tables**

Table 1. Effect of the supports on the catalytic performance of the PdRu bimetallic catalyst for Glycerol Hydrogenolysis. Product distribution and carbon mass balance of liquid product CMB (L) versus total carbon mass balance CMB (L+G).

| | | *Products Selectivity (%)* | | | | | | | | | | | | | | |
|---|---|---|---|---|---|---|---|---|---|---|---|---|---|---|---|---|
| *Catalyst* | *Conversion (%)* | Acetone | MeOH | EtOH | 2-PO | 1-PO | Acetol | 1,2-PDO | EG | 1,3-PDO | $CO_2$ | $CH_4$ | $C_2H_6$ | $C_3H_8$ | *CMB(L) (%)* | *CMB(L+G) (%)* |
| *1* | 7 | 0 | 0 | 1 | 0 | 10 | 1 | 82 | 3 | 0 | 0 | 3 | 1 | 0 | 94 | 96 |
| *2* | 23 | 0 | 2 | 0 | 9 | 5 | 0 | 33 | 26 | 4 | 0 | 11 | 9 | 2 | 93 | 96 |
| *3* | 17 | 0 | 2 | 0 | 9 | 5 | 0 | 22 | 25 | 1 | 0 | 31 | 2 | 3 | 98 | 100 |
| *4* | 21 | 0 | 1 | 0 | 11 | 5 | 0 | 17 | 22 | 1 | 0 | 35 | 3 | 5 | 97 | 100 |
| *5* | 62 | 0 | 2 | 0 | 8 | 3 | 0 | 9 | 14 | 0 | 0 | 54 | 5 | 6 | 61 | 81 |
| *6* | 51 | 0 | 1 | 0 | 8 | 2 | 0 | 14 | 15 | 1 | 0 | 49 | 5 | 5 | 77 | 96 |
| *7* | 72 | 0 | 1 | 0 | 7 | 2 | 0 | 17 | 9 | 0 | 0 | 53 | 5 | 6 | 64 | 92 |
| *8* | 20 | 0 | 2 | 0 | 10 | 3 | 0 | 16 | 27 | 1 | 0 | 37 | 2 | 3 | 98 | 100 |
| *9* | 10 | 0 | 2 | 1 | 0 | 9 | 0 | 53 | 31 | 0 | 0 | 3 | 1 | 0 | 99 | 100 |

*2 wt. % PdRu supported on 1) $Ti_{0.9}W_{0.1}O_2$, 2) $TiO_2$, 3) HY (5.1:1), 4) MOR (20:1), 5) ZSM-5 (30:1), 6) ZSM-5 (50:1), 7) ZSM-5 (80:1), 8) ZSM-5 (400-200:1), 9) $SiO_2$. Reaction conditions 165 $^oC$; $pH_2$: 20 bar, 800 rpm, 5h; glycerol to metal molar ratio of [1:0.005]*

Table 2. Effect of the supports on the catalytic performance of the PdRu bimetallic catalyst for Glycerol Hydrogenolysis. Product distribution and carbon mass balance of liquid product CMB (L) versus total carbon mass balance CMB (L+G).

| | | *Products Selectivity (%)* | | | | | | | | | | | | | | |
|---|---|---|---|---|---|---|---|---|---|---|---|---|---|---|---|---|
| *Catalyst* | *Conversion (%)* | Acetone | MeOH | EtOH | 2-PO | 1-PO | Acetol | 1,2-PDO | EG | 1,3-PDO | $CO_2$ | $CH_4$ | $C_2H_6$ | $C_3H_8$ | *CMB(L) (%)* | *CMB(L+G) (%)* |
| *1* | 12 | 0 | 0 | 0 | 0 | 5 | 0 | 49 | 2 | 0 | 1 | 19 | 6 | 18 | 96 | 101 |
| *2* | 55 | 0 | 2 | 1 | 0 | 1 | 0 | 49 | 19 | 0 | 0 | 24 | 3 | 1 | 72 | 83 |
| *3* | 89 | 0 | 1 | 1 | 0 | 4 | 1 | 26 | 10 | 0 | 0 | 38 | 13 | 7 | 31 | 56 |
| *4* | 22 | 0 | 2 | 0 | 0 | 4 | 0 | 19 | 36 | 0 | 0 | 33 | 3 | 1 | 86 | 93 |
| *5* | 7 | 0 | 1 | 0 | 0 | 8 | 1 | 42 | 28 | 0 | 0 | 17 | 2 | 2 | 64 | 98 |

*2 wt. % PdRu supported on 1) $Ti_{0.9}W_{0.1}O_2$, 2) $TiO_2$, 3) ZSM-5 (80:1), 4) $Al_2O_3$, 5) $SiO_2$. Reaction conditions 165 $^oC$; $pH_2$: 20 bar, 800 rpm, 16h; glycerol to the metal molar ratio of [1:0.005].*

**Figures**

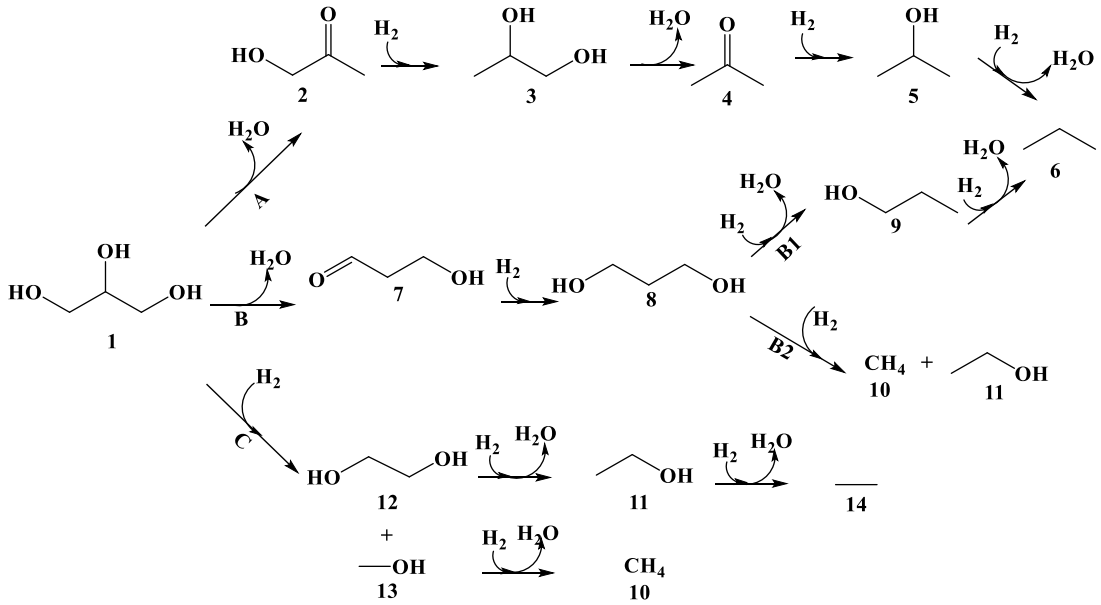


Scheme 1 Schematic representation of the glycerol hydrogenolysis reaction pathways. Compounds labelled as: 1) glycerol, 2) acetol, 3) 1,2-propanediol, 4) acetone, 5) 2-propanol, 6) propane, 7) 3-hydroxypropanaldehyde, 8) 1,3-propanediol, 9) 1-propanol, 10) methane, 11) ethanol, 12) ethylene glycol, 13) methanol, 14) ethane. Adapted from references [14, 50]

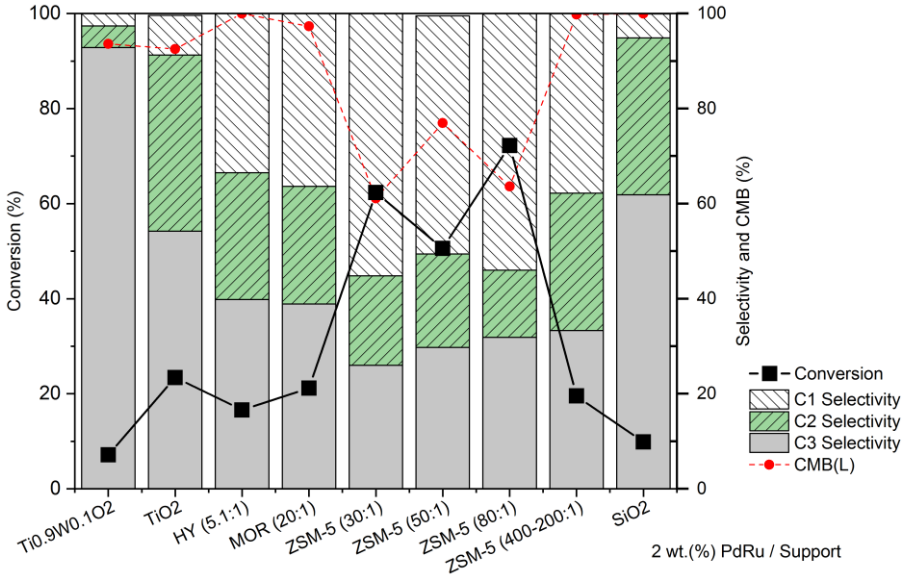


Figure 1. Effect of the support on the activity and selectivity using a 2 wt.% PdRu/support catalyst tested using as a molar ratio 1: 0.005 glycerol-metal and reaction conditions of 165 °C, 20 bar $H_2$, 800 rpm. Conversion (-■-), carbon mass balance (L) (- -●- -) and selectivity of products labelled as C1 ( ), C2 ( ), C3 ( ).

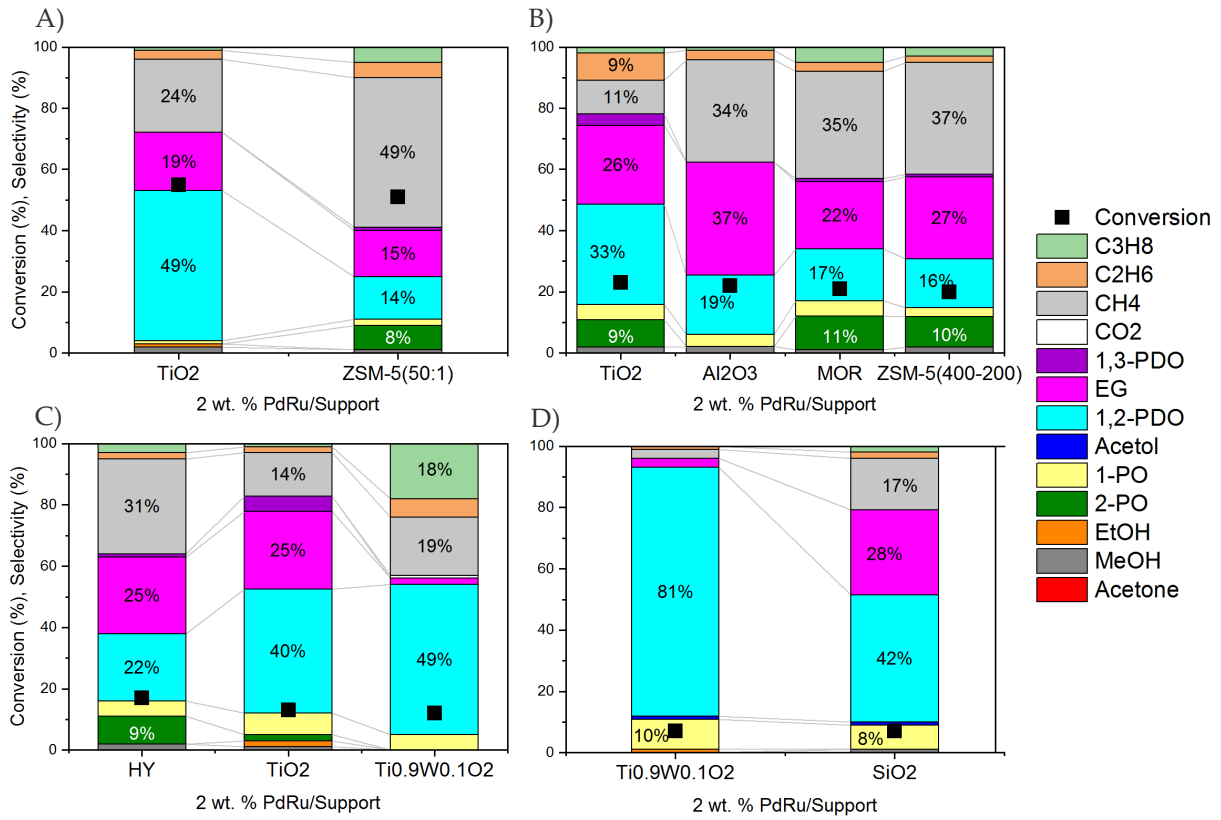


Figure 2. Distribution of the hydrogenolysis products at iso-conversion values (■) of A) 50-55 %, B) 20-25 %, C) 15-20 % and D) 5-10 %. Using 2 wt. % PdRu/support catalyst tested using as a molar ratio 1: 0.005 glycerol-metal and reaction conditions of 165 °C, 20 bar $H_2$, 800 rpm.

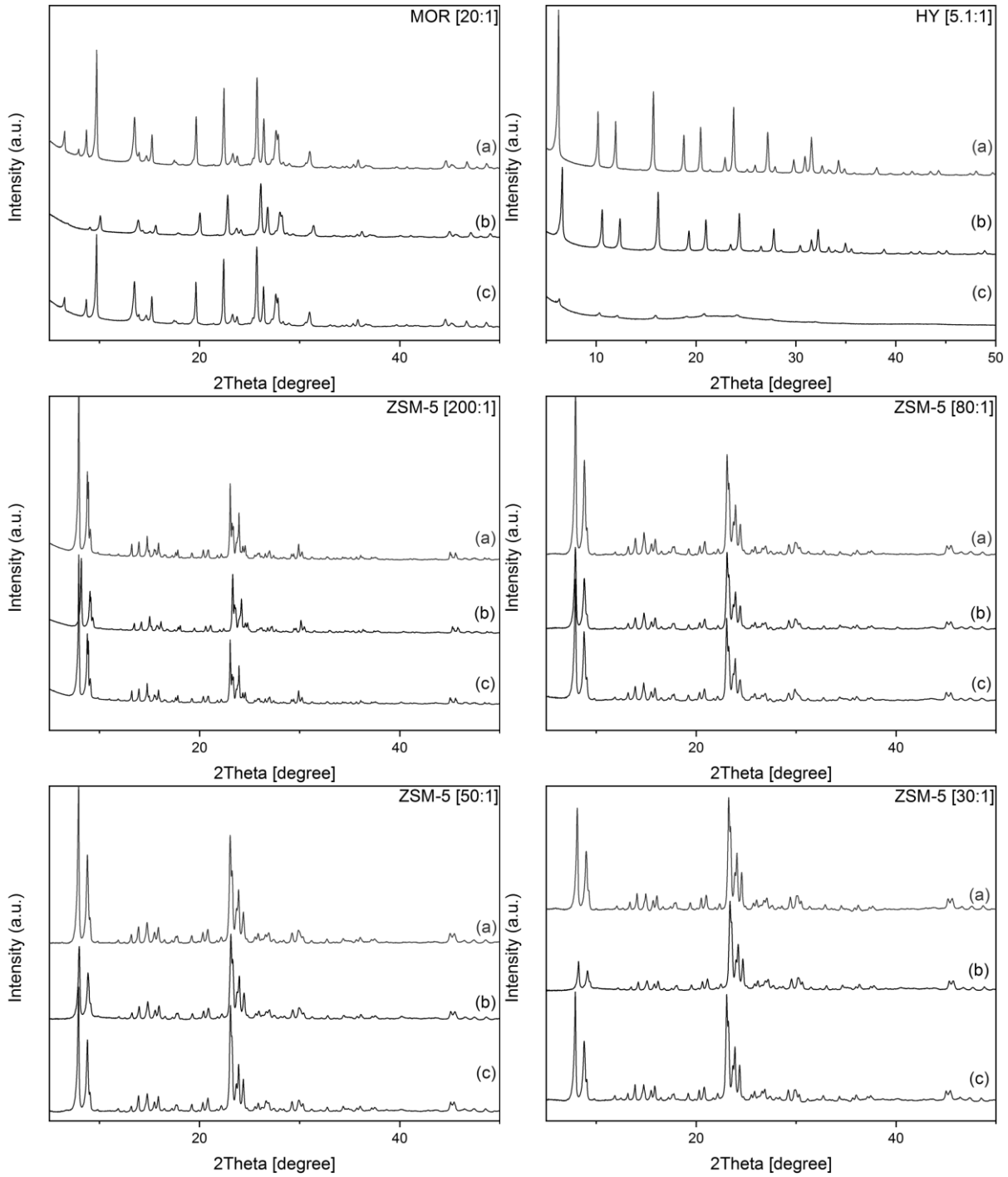


Figure 3. XRD diffractograms of the a) calcined b) fresh and c) spent catalysts

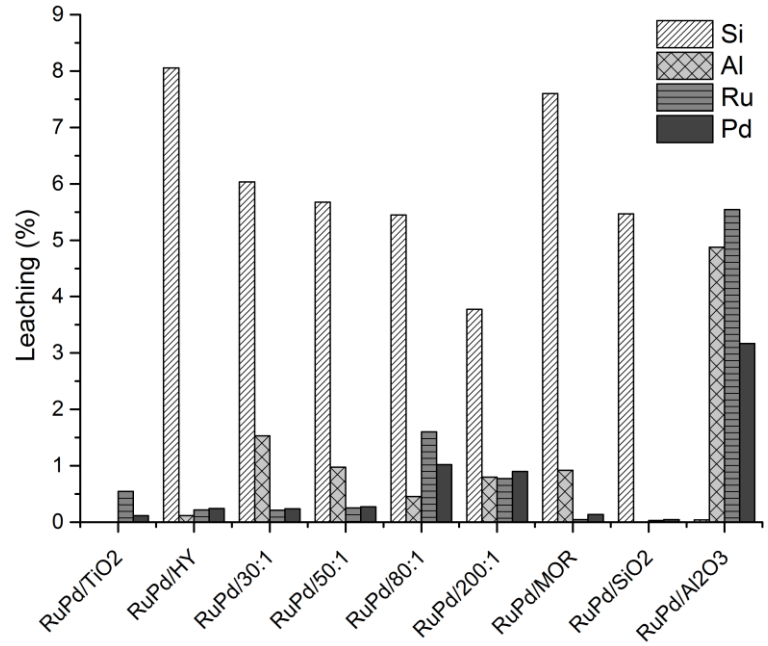


Figure 4 Leaching study by the analysis of reaction mixtures by ICP – MS.

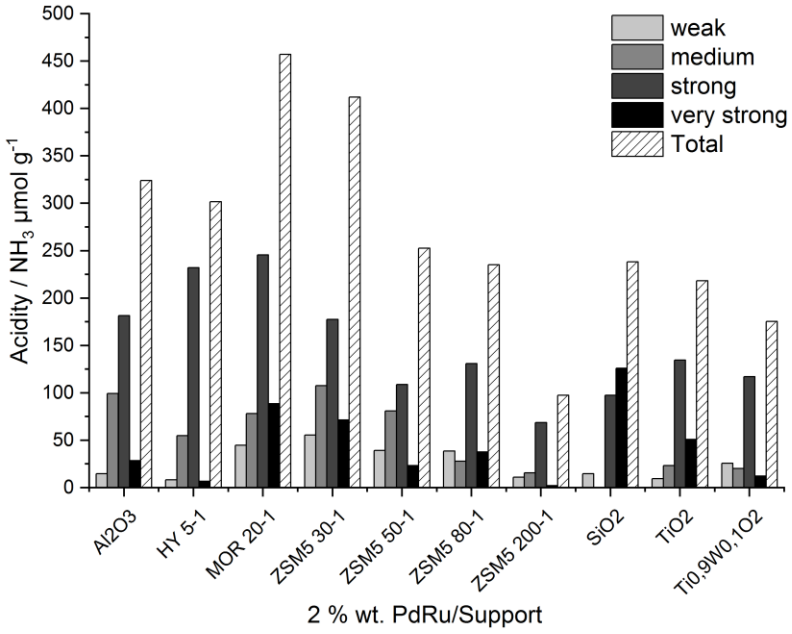


Figure 5. Acid site density distribution of the different bimetallic PdRu catalysts tested for the hydrogenolysis of glycerol

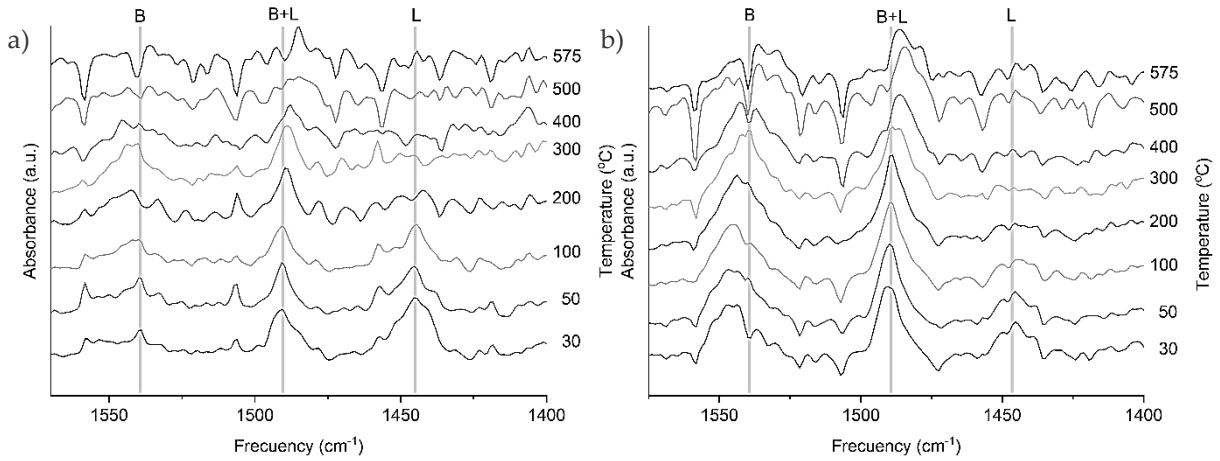


Figure 6. FTIR spectra of pyridine adsorbed on the materials recorded between 30-575 ºC. a) ZSM-5 (80:1), b) Mordenite (20:1).

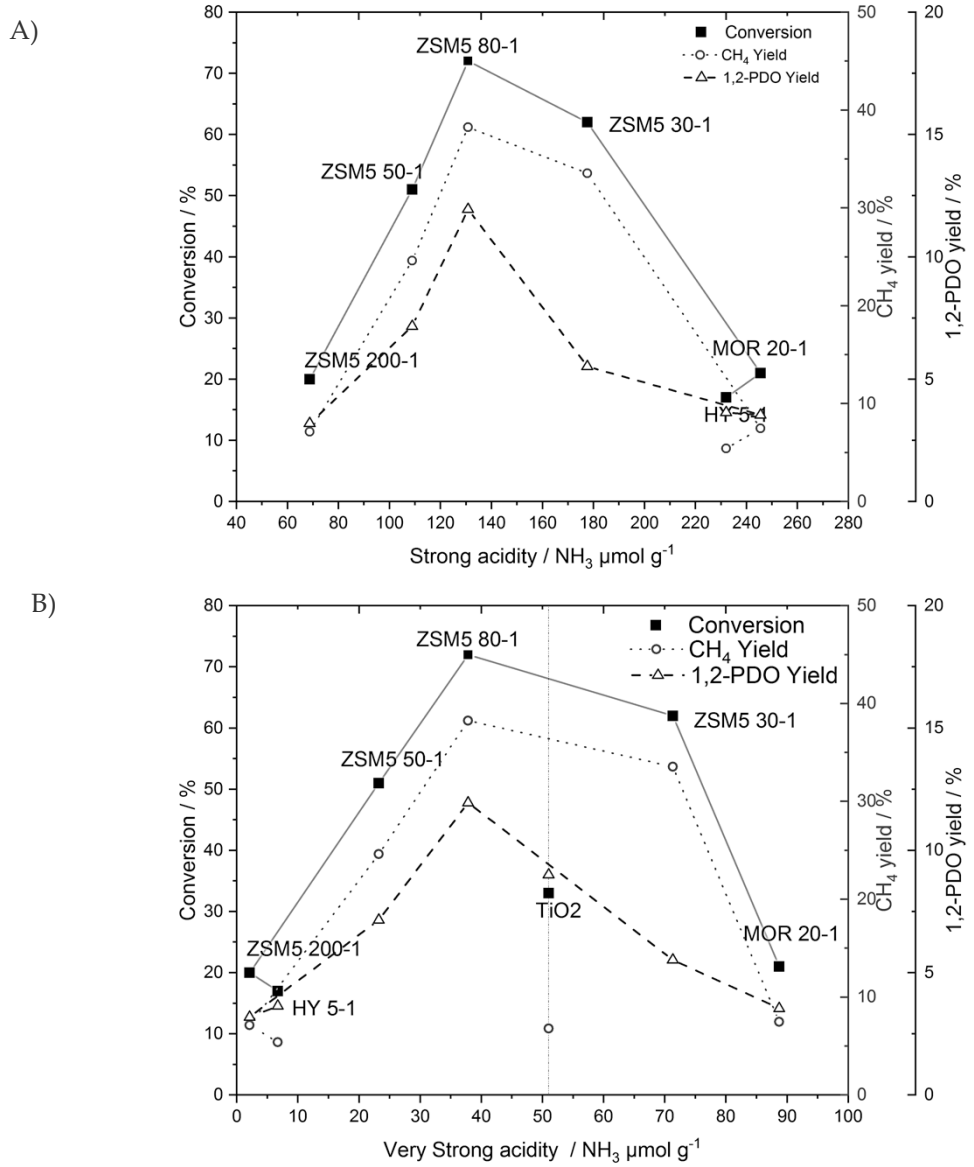

Figure 7. Volcano plot correlation between activity (conversion (■), $CH_4$ yield (○) and 1,2-PDO yield (Δ)) vs A) strong acidity sites estimated from ammonia desorption peak 3; and B) the very strong acidity sites obtained from ammonia desorption peak 4 (See *Supplementary Information*)